Radiology

ORIGINAL RESEARCH • MUSCULOSKELETAL IMAGING

Comparison of Whole-Body MRI, CT, and Bone Scintigraphy for Response Evaluation of Cancer Therapeutics in Metastatic Breast Cancer to Bone

Michael Kosmin, MBBS • Anwar R. Padhani, MBBS • Andrew Goghashian, MBBS • David Woolf, MBChB • Mei-Lin Ah-See, MBChB • Peter Ostler, MBBS • Stephanie Sutherland, MBBS • David Miles, MBBS • Jillian Noble, MBChB • Dow-Mu Koh, MD • Andrea Marshall, PhD • Janet Dunn, PhD • Andreas Makris, MBChB

From the Department of Oncology, University College London NHS Foundation Trust, 250 Euston Road, London NW1 2PG, England (M.K.); Paul Strickland Scanner Centre (A.R.P., A.G.) and Breast Cancer Research Unit (P.O., S.S., D.M., A. Makris), Mount Vernon Cancer Centre, Northwood, Middlesex, England; Department of Clinical Oncology, the Christie NHS Foundation Trust, Manchester, England (D.W.); Astra Zeneca UK Limited, Cambridge, England (M.L.A.); the Royal Marsden Hospital, Sutton, Surrey, England (J.N., D.M.K.); and Warwick Clinical Trials Unit, University of Warwick, Coventry, England (A. Marshall, J.D.). Received December 6, 2019; revision requested January 31, 2020; revision received August 14; accepted August 27. **Address correspondence to** M.K. (e-mail: *michael.kosmin@nhs.net*).

Supported by the Paul Strickland Scanner Centre Charity (UK registered charity number 298867) and Fighting Breast Cancer (UK registered charity number 1091882).

Conflicts of interest are listed at the end of this article.

Radiology 2020; 00:1–8 • https://doi.org/10.1148/radiol.2020192683 • Content codes: MK OI

Background: CT and bone scintigraphy have limitations in evaluating systemic anticancer therapy (SACT) response in bone metastases from metastatic breast cancer (MBC).

Purpose: To evaluate whether whole-body MRI enables identification of progressive disease (PD) earlier than CT and bone scintigraphy in bone-only MBC.

Materials and Methods: This prospective study evaluated participants with bone-only MBC between May 2016 and January 2019 (ClinicalTrials.gov identifier: NCT03266744). Participants were enrolled at initiation of first or subsequent SACT based on standard CT and bone scintigraphy imaging. Baseline whole-body MRI was performed within 2 weeks of entry; those with extraosseous disease were excluded. CT and whole-body MRI were performed every 12 weeks until definitive PD was evident with one or both modalities. In case of PD, bone scintigraphy was used to assess for bone disease progression. Radiologists independently interpreted images from CT, whole-body MRI, or bone scintigraphy and were blinded to results with the other modalities. Systematic differences in performance between modalities were analyzed by using the McNemar test.

Results: Forty-five participants (mean age, 60 years ± 13 [standard deviation]; all women) were evaluated. Median time on study was 36 weeks (range, 1–120 weeks). Two participants were excluded because of unequivocal evidence of liver metastases at baseline whole-body MRI, two participants were excluded because they had clinical progression before imaging showed PD, and one participant was lost to follow-up. Of the 33 participants with PD at imaging, 67% (22 participants) had PD evident at whole-body MRI only and 33% (11 participants) had PD at CT and whole-body MRI concurrently; none had PD at CT only ($P < .001$, McNemar test). There was only slight agreement between whole-body MRI and CT (Cohen κ, 0.15). PD at bone scintigraphy was reported in 50% of participants (13 of 26) with bone progression at CT and/or whole-body MRI ($P < .001$, McNemar test).

Conclusion: Whole-body MRI enabled identification of progressive disease before CT in most participants with bone-only metastatic breast cancer. Progressive disease at bone scintigraphy was evident in only half of participants with bone progression at whole-body MRI.

Online supplemental material is available for this article.

Despite the fact that bone is the most common site for metastases from breast cancer (1), standard imaging modalities have substantial limitations in the identification of metastatic bone disease and assessment of treatment response. In Response Evaluation Criteria in Solid Tumors version 1.1, bone metastases are considered nonmeasurable lesions (2), and increased sclerosis and sclerotic response of bone metastases can be difficult to distinguish with CT (3). Bone scintigraphy with technetium 99m (^{99m}Tc)–methylene diphosphonate often results in underestimation of disease extent, and difficulties in interpretation of serial bone scans are well described (3,4). Fluorine 18 fluorodeoxyglucose (FDG) PET allows for identification of changes in metabolic activity related to glucose uptake. Changes in maximum FDG standardized uptake value are predictive of duration of treatment response and time to progression (5,6). However, a proportion of bone metastases can be FDG negative and not identifiable at FDG PET imaging (7,8).

Recently, there has been renewed interest in the use of whole-body MRI with diffusion-weighted sequences as a method for assessing malignant disease of bone. Whole-body MRI is used to evaluate bone and soft-tissue disease directly, and there is no requirement for injected contrast agents or exposure to ionizing radiation. Benign and malignant lesions can be differentiated on the basis of differences in cellular density and changes in water diffusivity, providing early signs of disease response

Abbreviations

FDG = fluorine 18 fluorodeoxyglucose, MBC = metastatic breast cancer, PD = progressive disease, SACT = systemic anticancer therapy

Summary

In participants receiving systemic anticancer therapy for bone-only metastatic breast cancer, whole-body MRI enabled identification of progressive disease earlier than whole-body CT and bone scintigraphy.

Key Results

- Whole-body MRI depicted disease progression before CT in 67% of participants (22 of 33) with bone-only metastatic breast cancer ($P < .001$), with only slight agreement between the two modalities ($\kappa = 0.15$).
- Bone scintigraphy revealed progression in only 50% of participants (13 of 26) with bone progression identified with whole-body MRI ($P < .001$).

or progression (9). Whole-body MRI is now an established tool in the diagnosis and assessment of multiple myeloma (10–12), and there are published practical guidelines for the acquisition, interpretation, and reporting of whole-body MRI scans in patients with multiple myeloma and advanced prostate cancer (13,14).

There is limited literature investigating the role of whole-body MRI in clinical decision making in metastatic breast cancer (MBC). Retrospective data show that whole-body MRI often depicts sites of disease not evident on CT images, and that systemic anticancer therapy (SACT) changes are made based on evidence of progressive disease (PD) seen only at whole-body MRI in more than one-third of cases (15). There is also evidence for the superior performance of whole-body MRI compared with FDG PET/CT for SACT response assessment (16).

The primary objective of this prospective study was to evaluate whether whole-body MRI depicts PD earlier than CT and bone scintigraphy in bone-only MBC. We hypothesized that whole-body MRI would enable identification of PD earlier than CT in this patient group.

Materials and Methods

All procedures performed in this study (ClinicalTrials.gov identifier: NCT03266744) were in accordance with the ethical standards of the National Health Service Health Research Authority East of England–Cambridge East Research Ethics Committee and with the 1964 Helsinki Declaration and its later amendments or comparable ethical standards. This work was funded by the Paul Strickland Scanner Centre Charity (UK registered charity number 298867) and Fighting Breast Cancer (UK registered charity number 1091882). Written informed consent was obtained from all participants included in the study. M.L.A. has been an employee of AstraZeneca UK Limited since April 2018 and is a current shareholder. This affiliation does not lead to a direct conflict of interest with the presented work. The study protocol and data generated are available from the corresponding author by request.

Study Participants

Participants were recruited as a consecutive series between May 2016 and June 2017 at Mount Vernon Cancer Center, Northwood, England, and the Royal Marsden Hospital, Sutton, England. Imaging was performed until database cutoff in January 2019. Eligible participants had documented bone-only MBC, as established with standard CT and bone scintigraphy performed no more than 4 weeks before trial entry, and were starting SACT de novo or a new line of SACT. Inclusion criteria included a histologic diagnosis of breast cancer in patients with single or multiple bone metastases without extraosseous or nonbone metastatic disease. Participants were required to be aged 18 years or older with no other current active malignancy and a life expectancy greater than 6 months. Patients were excluded from the study if they were to undergo radical treatment (eg, surgery or stereotactic radiation therapy) to a sole site of metastatic disease. Pregnant patients were excluded. The usual contraindications to MRI were also applied, including cardiac pacemakers and neurostimulators and marked claustrophobia. Metal implants in bone and/or breast prostheses were not a contraindication. Baseline whole-body MRI was performed within 2 weeks of study entry. No further imaging tests were performed to evaluate disease burden, but any additional tests required for the initiation of the new SACT, such as blood work-up or electrocardiography or echocardiography, were performed according to local protocols.

During the study, CT and whole-body MRI were performed every 12 weeks (±7 days) until PD was evident. If there was equivocal evidence of PD at whole-body MRI only, repeat whole-body MRI was undertaken 4–6 weeks later to confirm or refute the presence of definite PD. If PD was confirmed, then the date of progression was defined as that of the whole-body MRI examination performed 4–6 weeks earlier. No repeat CT examinations were performed in addition to the confirmatory whole-body MRI.

The end of the study protocol for an individual participant was reached when any of the following occurred: unequivocal progressive bone and/or visceral (including lung) disease was demonstrated at CT scan and whole-body MRI; unequivocal progressive bone and/or visceral disease was demonstrated at CT or whole-body MRI alone; or CT and/or whole-body MRI findings and/or clinical disease progression necessitated intervention such as palliative radiation therapy or a change in systemic therapy. Repeat bone scintigraphy was performed when the participant met one of the end-of-study criteria. Findings were compared with those from baseline bone scintigraphy to assess for evidence of PD.

Whole-body MRI protocol.—Imaging was performed at both centers with a Magnetom Avanto Fit scanner (Siemens Healthineers, Erlangen, Germany) by using methods compliant with the Metastasis Reporting and Data System for Prostate Cancer and the Myeloma Response Assessment and Diagnosis System standards for whole-body MRI in bone disease evaluations (13,14). Integrated posterior spine and head and neck coils were used. Two linked, anterior body 18-coil arrays

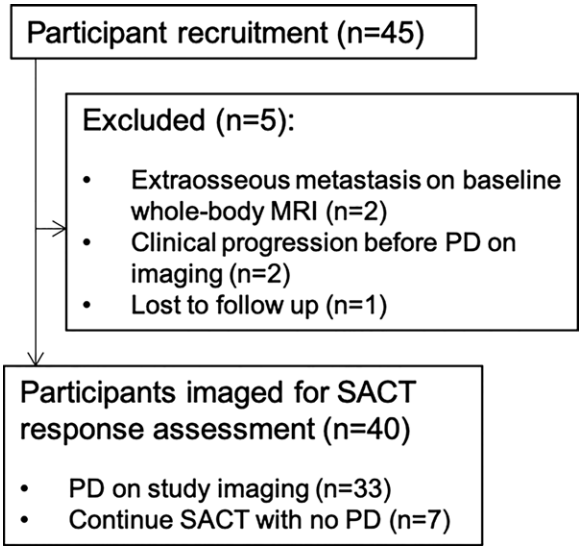

Figure 1: Flowchart shows number of participants recruited and number and reasons for exclusion from study. PD = progressive disease, SACT = systemic anticancer therapy.

were used for coverage of the chest, abdomen, and pelvis to the midthighs. Peripheral coils were not used. The following sequences were included for whole spine imaging: *(a)* sagittal T1-weighted turbo spin-echo imaging with 4-mm-thick slices in two stations and *(b)* sagittal short inversion time inversion-recovery T2-weighted imaging with 4-mm-thick slices in two stations. The following sequences were used for whole-body imaging (skull base to midthighs): axial and coronal T1-weighted gradient-recalled echo imaging with a Dixon technique with fat percentage reconstructions. The following sequences were used for whole-body imaging from vertex to midthighs: axial, diffusion-weighted, short inversion time inversion-recovery imaging with fat suppression, 5-mm contiguous slicing, in four contiguous stations by using *b* values of 50, 600, and 900 sec/mm^2. Apparent diffusion coefficient calculations were performed in-line with monoexponential data fitting to the signal intensities of the above *b*-value images. Other reconstructions included coronal multiplanar reconstructions (as contiguous two-dimensional 5-mm-thick slices) with a *b* value of 900 sec/mm^2 and whole-body three-dimensional maximum intensity projection reconstructions with a *b* value of 900 sec/mm^2 with images displayed as rotating images with inverted gray scale. Whole-body (skull base to midthighs) axial T2-weighted, turbo spin-echo imaging without fat suppression, with 5-mm-thick contiguous slices in multiple stations, was also performed, matching the diffusion-weighted images. Scheduling time was 60 minutes; acquisition time, including setup, adjustments, and sequences, was 55 minutes. Full sequence parameters can be found in Table E1 (online).

CT protocol.—CT was performed at both study sites with a Siemens Somatom Force scanner in dynamic mode. Optiray 350 (Guerbet, Princeton, NJ) intravenous contrast agent was used (75 mL for participants weighing <80 kg; otherwise, 100 mL) with the patient in a supine position with arms raised. The field of view extended from the midcervical spine to the midfemora. Imaging of the chest and abdomen was performed in the arterial phase with triggering at the peak arterial phase (5 seconds after peak pulmonary artery), and the abdomen and pelvis were examined in the portal phase, 35 seconds later. Two-millimeter soft-tissue, lung, and bone reconstructions were undertaken with appropriate windowing and kernels.

Breast Cancer Characteristics and SACT Information for Study Participants

Parameter	No. of Participants
Histologic finding	
Invasive ductal carcinoma	34 (76)
Invasive lobular carcinoma	8 (18)
Mixed	2 (4.4)
Unknown	1 (2.2)
Grade	
1	4 (8.9)
2	23 (51)
3	16 (36)
Unknown	2 (4.4)
Estrogen receptor status	
Positive	40 (89)
Negative	5 (11)
Unknown	0 (0)
HER2 status	
Positive	4 (8.9)
Negative	41 (91)
Unknown	0 (0)
Line of SACT (for metastatic breast cancer)	
1	25 (56)
2	10 (22)
3	7 (16)
4	2 (4.4)
5	1 (2.2)
Type of SACT	
Chemotherapy	12 (27)
Hormonal therapy	33 (73)
With HER2-targeted therapy	3 (6.7)

Note.—Data are numbers of participants, with percentages in parentheses. The mean age of study participants was 60 years ± 13 (standard deviation); all participants were women. HER2 = human epidermal growth factor 2, SACT = systemic anticancer therapy.

Bone scintigraphy protocol.—Imaging was performed with a SKYLight system (Philips, Amsterdam, the Netherlands) at Mount Vernon Cancer Center and with a Siemens Intevo scanner at the Royal Marsden Hospital; both are dual-headed gamma cameras. Imaging was performed between 2.5 and 3 hours after intravenous injection of 600 MBq of ^{99m}Tc–methylene diphosphonate. Only planar imaging in the anterior and posterior planes of the whole body was undertaken without regional spot views or SPECT reconstructions.

Imaging Evaluation

Objective tumor response was evaluated separately for CT and whole-body MRI scans by dedicated oncological radiologists

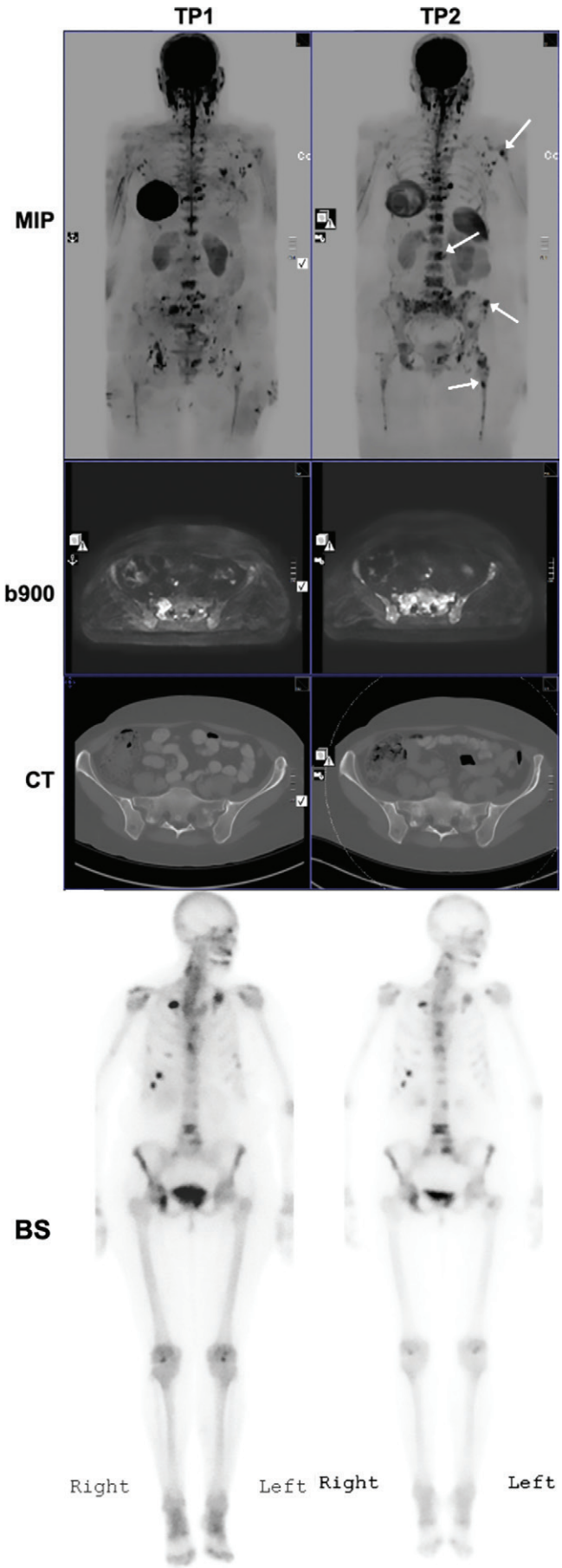

Figure 2: Images show differences between whole-body MRI, CT, and bone scintigraphy in depicting sites of bone progression in 59-year-old woman with estrogen receptor–positive, human epidermal growth factor receptor 2–negative grade 1 invasive ductal carcinoma. The patient was receiving fulvestrant as third-line systemic anticancer therapy for metastatic breast cancer. Baseline imaging was performed in in August 2016 (time point 1 [TP1]); response assessment imaging was performed in March 2017 (time point 2 [TP2]). Coronal high-signal-intensity inverted maximum intensity projection (MIP) images obtained with whole-body MRI show progressive disease (PD) at multiple bone sites (arrows). Progression at these sites is not apparent on scans obtained at bone scintigraphy (BS) (anterior planar view). PD is also evident on axial MRI scans obtained through the sacrum with *b* value of 900 sec/mm^2 (b900). Changes in mineralization on axial CT images through sacrum do not meet criteria for PD.

(A.R.P., A.G., or D.M.K.) with more than 10 years of experience in interpreting whole-body MRI and CT scans. A.R.P. and D.M.K. have been involved in the formulation of the whole-body MRI Metastasis Reporting and Data System for Prostate Cancer (13) and Myeloma Response Assessment and Diagnosis System (14) guidelines and have led formal training of radiologists in whole-body MRI. Different readers (A.R.P., A.G., or D.M.K.) interpreted the whole-body MRI and CT scans. Bone scintigraphy findings were reported by separate nuclear medicine radiologists. The MRI and CT readers were blinded to the imaging results of the other modality; the bone scintigraphy reader was aware of the presence of PD. Imaging evaluations were done at the patient level with no separate analyses by sequence or anatomic region. Details of the imaging criteria for disease response evaluation can be found in Appendix E1 (online).

Statistical Design

This nonrandomized study was designed to detect a superiority in performance of whole-body MRI versus CT in the identification of first PD. With use of an A'Hern single-stage phase II procedure with 90% power and a one-sided α of .05, 33 evaluable participants were required in order to determine an improvement in identification of first PD by means of whole-body MRI from 50% to 75% of participants. Statistical analysis comparing the proportion of first PD identified by means of whole-body MRI alone versus CT alone versus concurrent PD in both modalities was performed by using the McNemar test to detect systematic differences in performance. The Cohen κ test was used to evaluate the overall level of agreement between whole-body MRI and CT. Database cutoff occurred when all enrolled participants had been in the study for at least 36 weeks or had reached the end of the aforementioned study protocol. $P < .05$ was considered to indicate a statistically significant difference in all tests. Statistical analysis was performed with software (StatsDirect Statistical Software, version 3, 2019; StatsDirect, Cheshire, England).

Results

Participant Characteristics

Forty-five participants were recruited (Fig 1). The mean age of all participants was 60 years (standard deviation, 13 years;

all women). Most participants (56%; 25 of 45 participants) were enrolled at the point of initiation of first-line SACT for MBC. A summary of the breast cancer characteristics and SACTs of the participants is shown in the Table.

Of the 33 participants receiving hormonal therapy, four received additional ovarian suppression with goserelin. One participant started everolimus alongside exemestane. Three participants received cyclin-dependent kinase 4 and 6 inhibitors (two received palbociclib; one received ribociclib) with aromatase inhibitors. Of the three participants receiving human epidermal growth factor receptor 2–targeted therapy, one received trastuzumab emtansine, one received trastuzumab with capecitabine, and one received trastuzumab with exemestane.

Of the 45 participants, two (4.4%) with bone-only disease at CT and bone scintigraphy before trial entry had unequivocal evidence of liver metastases on their baseline whole-body MRI scans. Their involvement in the study ceased at that point. Two participants (4.4%) had clinical PD requiring SACT change before evidence of PD at study imaging. One participant moved abroad and was classified as lost to follow-up. A total of 129 pairs of CT and whole-body MRI scans were performed for response assessment. Median participant time on study was 36 weeks (range, 1–120 weeks).

At the time of database cutoff, the remaining 40 participants had either met the primary end point of PD at imaging (n = 33) or continued with the SACT initiated at trial entry with no evidence of PD at their most recent imaging time point (n = 7). The median time to reported PD was 24 weeks (range, 12–84 weeks). One participant required early reassessment whole-body MRI

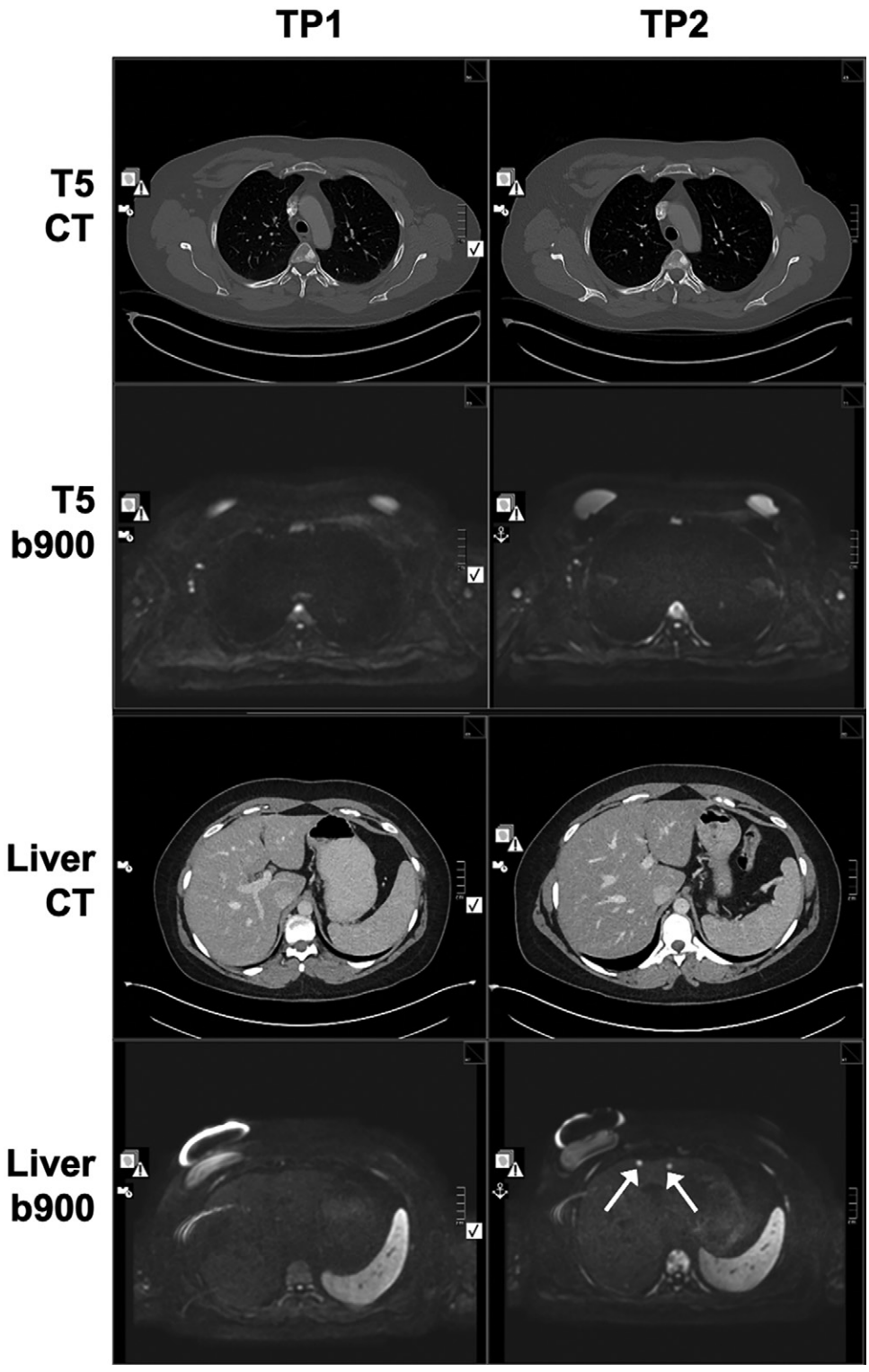

Figure 3: Images show disease progression in bone and liver seen only at whole-body MRI in 36-year-old woman with estrogen receptor–positive, human epidermal growth factor receptor 2–negative grade 3 invasive ductal carcinoma. The patient was receiving eribulin chemotherapy and denosumab as fourth-line systemic anticancer therapy for metastatic breast cancer. Baseline imaging was performed in August 2016 (time point 1 [TP1]); response assessment imaging was performed in February 2017 (time point 2 [TP2]). Evidence of progressive disease of bone lesion in T5 vertebral body is seen on axial high-signal-intensity (*b* value, 900 sec/mm^2) whole-body MRI scan (b900); however, no change is seen in CT image at level of T5. Multiple new liver lesions (arrows) are evident on axial MRI scan obtained with *b* value of 900 sec/mm^2 but do not appear on CT image.

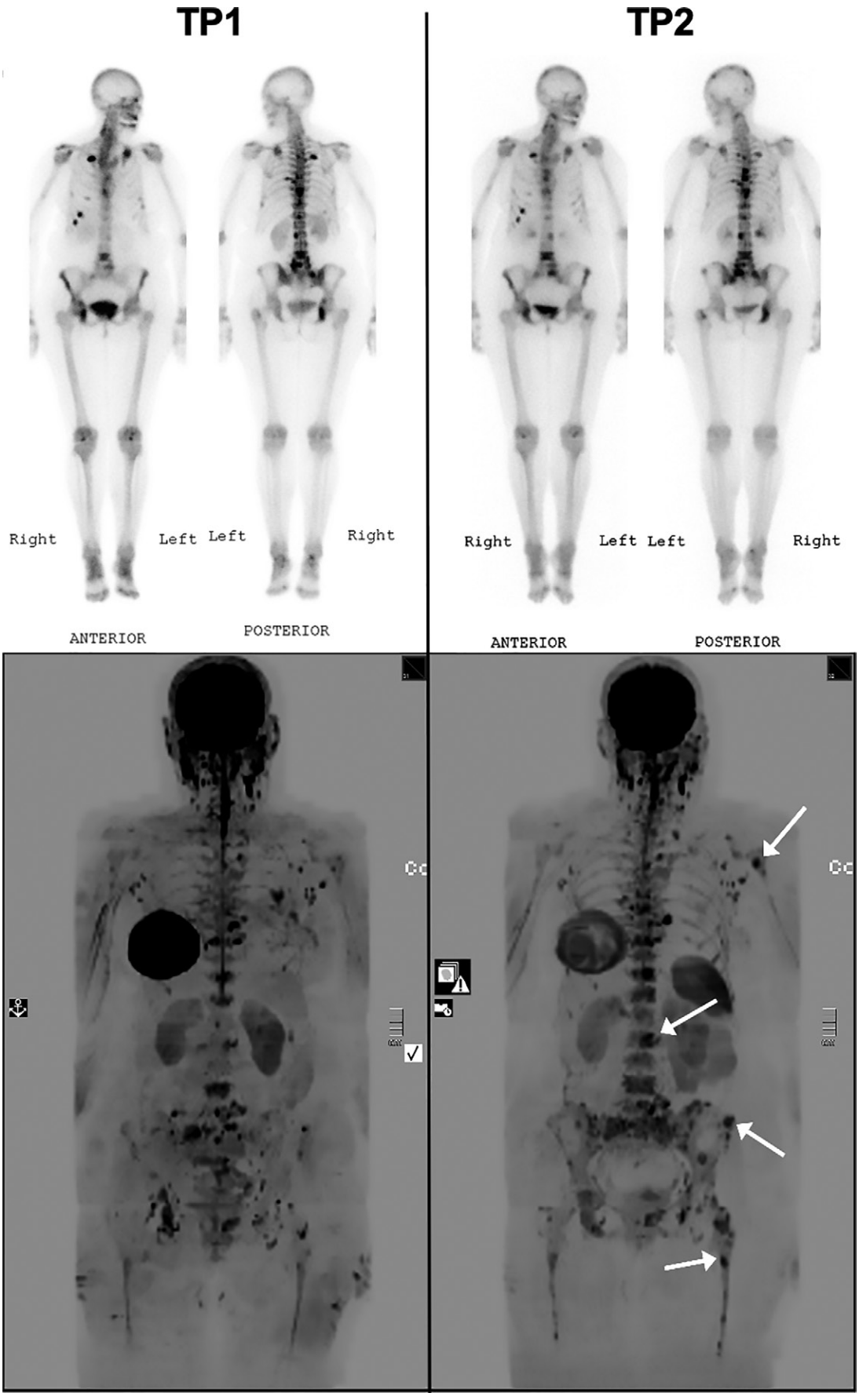

Figure 4: Images show discordance between bone scintigraphy and whole-body MRI in 36-year-old woman with estrogen receptor–positive, human epidermal growth factor receptor 2–negative grade 3 invasive ductal carcinoma. The patient was receiving eribulin chemotherapy and denosumab as fourth-line systemic anticancer therapy for metastatic breast cancer. Baseline imaging was performed in August 2016 (time point 1 [TP1]); response assessment imaging was performed in February 2017 (time point 2 [TP2]). Coronal images from bone scintigraphy (top) and inverted maximum intensity projection images obtained with a *b* value of 900 sec/mm^2 at whole-body MRI (bottom) are shown. Whole-body MRI scan at response assessment imaging shows evidence of progressive disease at multiple bone sites (arrows). Image from bone scintigraphy does not show disease progression at these locations.

owing to equivocal changes of possible PD seen at whole-body MRI alone. In this case, repeat whole-body MRI performed 31 days later confirmed PD.

PD at Whole-Body MRI, CT, and Bone Scintigraphy

Among the 33 participants with PD at imaging, PD was evident only on whole-body MRI scans in 22 (67%). The remaining 11 participants (33%) had PD evident on both CT and whole-body MRI scans at the same time point. There were no participants with PD at CT alone. All 40 participants who met the primary end point of the study or who were still enrolled at database cutoff were included in the McNemar analysis. The contingency table incorporated the following groups: PD at both whole-body MRI and CT (n = 11); PD at whole-body MRI alone (n = 22); PD at CT alone (n = 0); and PD at neither whole-body MRI nor CT (n = 7). Performance between CT and whole-body MRI differed in identification of PD ($P < .001$, McNemar test). The Cohen κ statistic was 0.15 (95% confidence interval: 0.02, 0.27), suggesting only slight agreement between whole-body MRI and CT.

Of the 33 participants with PD at imaging, 25 (76%) had bone-only progression, five (15%) had PD in bone and at extraosseous sites concurrently (three with new liver metastases, two with new metastatic nodal disease), and three (9.1%) had extraosseous PD alone (one participant had liver-only PD; one had liver and lung PD; one had brain-only PD). Of the 22 participants in whom PD was seen only at whole-body MRI, 18 had bone-only PD (Fig 2), two had bone and liver PD (Fig 3), and two had extraosseous PD (one liver only, one brain only).

Of the 26 end-of-study bone scintigraphy procedures performed when there was PD in bone at CT and/or whole-body MRI, progression at bone scintigraphy was reported in 13 (50%) ($P < .001$, McNemar test). An example case of PD at whole-body MRI without PD at bone scintigraphy is shown in Figure 4. PD was not reported at bone scintigraphy in the three participants with extraosseous progression.

Overall, only 21% of participants (six of 29) had evidence of PD with all three modalities (whole-body MRI, CT, and bone scintigraphy). Forty-one percent of participants (12 of 29) had PD evident at whole-body MRI only; 14% (four of 29) had PD at whole-body MRI and CT only; and 24% (seven of 29) had PD at whole-body MRI and bone scintigraphy only.

Discussion

Clinical management of patients with bone-only metastatic breast cancer (MBC) has been limited by the inability of bone scintigraphy and CT to reliably and accurately enable identification of progressive disease (PD). In our prospective study in which whole-body MRI and CT were compared for response assessment in patients with bone-only MBC, whole-body MRI enabled identification of PD before CT in 67% of participants ($P < .001$, McNemar test). Evidence of PD at bone scintigraphy was found in only 50% of participants with PD in bone identified with whole-body MRI ($P < .001$, McNemar test), providing further evidence of the poor performance of bone scintigraphy as a tool for response assessment in MBC. Levels of participant-reported tolerability and compliance with whole-body MRI were high in our trial, even after multiple scanning episodes.

There were several potential mechanisms for the differences in performance between the imaging modalities evaluated in this study. Unlike whole-body MRI, CT and bone scintigraphy are used to evaluate the bone matrix response to the presence of cancer cells rather than the metastatic foci themselves, meaning that they are indirect reporters of malignant bone marrow pathologic features. Progression within metastatic foci is therefore detectable with CT and bone scintigraphy only when there has been an appreciable change in the surrounding bone structure. In bone scintigraphy, detection of bone metastases is reliant on increased osteoblast activity in the vicinity of the metastases, which results in differential tracer accumulation at sites of mineral deposition. With CT, changes in bone mineralization due to disease progression causing bone destruction and/or new bone formation must become perceptible before PD can be identified (3). This limits the sensitivity of these modalities for assessing the response of bone metastases to treatment. Whole-body MRI enables direct evaluation of metastatic lesions in the bone marrow space, with changes in water diffusivity reflecting changes in cellularity within lesions and displacement of marrow fat providing earlier signs of disease progression (9).

Earlier identification of progression of MBC in bone may allow switching from a failing systemic therapy sooner, potentially facilitating better control of disease over time. Use of whole-body MRI may help identify patients at particular risk of symptomatic skeletal events such as metastatic spinal cord and/or cauda equina compression, pathologic fractures, and sites of bone pain necessitating palliative radiation therapy (17). However, it remains unclear whether earlier identification of disease progression with whole-body MRI and earlier change in SACT can lead to improved outcomes (eg, reduced rates of symptomatic skeletal events) in MBC. To our knowledge, there are no published data on the prognostic importance of the change in disease burden through multiple lines of SACT in MBC.

This study was limited by enrolling only patients with bone-only MBC. We therefore cannot comment on whether other patient subgroups (eg, those with locally advanced or nodal or visceral disease) would benefit equally from the use of whole-body MRI. We did not evaluate the disease detection sensitivity according to MRI sequence type, as our aim was to perform a patient-level analysis. Such analyses have been performed by other investigators for myeloma and prostate cancer (18). Our study was limited by the small number of participants and the use of different bone scintigraphy equipment at the two centers. However, CT and MRI equipment was identical, and common quality assurance and quality control procedures were in place for the two participating centers for both modalities. Another limitation of this study was the use of confirmatory whole-body MRI (but not CT) in cases of equivocal progression seen at whole-body MRI only 4–6 weeks earlier. However, this was undertaken in only one participant and is unlikely to alter the study findings.

Further investigation of whole-body MRI is required to establish whether its use as a SACT response assessment tool in patients with bone metastases from breast cancer improves clinical

outcomes, such as a reduction in the rate of symptomatic skeletal events. The development of consensus guidelines for the acquisition, interpretation, and reporting of whole-body MRI in MBC would deal with the current lack of widely recognized criteria for assessment of bone disease in MBC, although guidelines do exist for metastatic prostate cancer (13) and for multiple myeloma (14). Such guidelines would enable patients with bone-only MBC to enter future clinical trials of promising anticancer therapeutics through use of whole-body MRI for more accurate and reliable assessment of their bone disease status.

In conclusion, whole-body MRI enabled identification of progressive disease (PD) before CT in most participants with bone-only metastatic breast cancer. PD at bone scintigraphy was evident in only half of participants with bone progression at whole-body MRI.

Author contributions: Guarantors of integrity of entire study, M.K., A.R.P., D.M., A. Makris; study concepts/study design or data acquisition or data analysis/interpretation, all authors; manuscript drafting or manuscript revision for important intellectual content, all authors; approval of final version of submitted manuscript, all authors; agrees to ensure any questions related to the work are appropriately resolved, all authors; literature research, M.K., A.R.P., A.G., D.W., M.L.A., P.O., A. Makris; clinical studies, M.K., A.R.P., A.G., D.W., P.O., D.M., J.N., J.D., A. Makris; experimental studies, D.W., P.O., A. Makris; statistical analysis, M.K., A.R.P., P.O.,D.M., A. Marshall, J.D., A. Makris; and manuscript editing, M.K., A.R.P., A.G., P.O., D.M., D.M.K., A. Marshall, A. Makris.

Disclosures of Conflicts of Interest: **M.K.** disclosed no relevant relationships. **A.R.P.** disclosed no relevant relationships. **A.G.** Activities related to the present article: received support for travel/accommodations and meeting expenses from Paul Strickland Scanner Centre. Activities not related to the present article: received support for travel/accommodations and meeting expenses from Paul Strickland Scanner Centre. Other relationships: disclosed no relevant relationships. **D.W.** disclosed no relevant relationships. **M.L.A.** Activities related to the present article: disclosed no relevant relationships. Activities not related to the present article: has been employed by AstraZeneca since April 2018, however involvement in this study predates this employment and AstraZeneca had no involvement in the study; has stock/stock options in AstraZeneca. Other relationships: disclosed no relevant relationships. **P.O.** disclosed no relevant relationships. **S.S.** disclosed no relevant relationships. **D.M.** disclosed no relevant relationships. **J.N.** disclosed no relevant relationships. **D.M.K.** disclosed no relevant relationships. **A. Marshall** disclosed no relevant relationships. **J.D.** disclosed no relevant relationships. **A. Makris** disclosed no relevant relationships.

References

1. Front D, Schneck SO, Frankel A, Robinson E. Bone metastases and bone pain in breast cancer. Are they closely associated? JAMA 1979;242(16):1747–1748.
2. Eisenhauer EA, Therasse P, Bogaerts J, et al. New response evaluation criteria in solid tumours: revised RECIST guideline (version 1.1). Eur J Cancer 2009;45(2):228–247.
3. Woolf DK, Padhani AR, Makris A. Assessing response to treatment of bone metastases from breast cancer: what should be the standard of care? Ann Oncol 2015;26(6):1048–1057.
4. Coleman RE, Fogelman I, Rubens RD. Hypercalcaemia and breast cancer: an increased humoral component in patients with liver metastases. Eur J Surg Oncol 1988;14(5):423–428.
5. Tateishi U, Gamez C, Dawood S, Yeung HWD, Cristofanilli M, Macapinlac HA. Bone metastases in patients with metastatic breast cancer: morphologic and metabolic monitoring of response to systemic therapy with integrated PET/CT. Radiology 2008;247(1):189–196.
6. Specht JM, Tam SL, Kurland BF, et al. Serial 2-[18F] fluoro-2-deoxy-D-glucose positron emission tomography (FDG-PET) to monitor treatment of bone-dominant metastatic breast cancer predicts time to progression (TTP). Breast Cancer Res Treat 2007;105(1):87–94.
7. Al-Muqbel KM, Yaghan RJ, Al-Omari MH, Rousan LA, Dagher NM, Al Bashir S. Clinical relevance of 18F-FDG-negative osteoblastic metastatic bone lesions noted on PET/CT in breast cancer patients. Nucl Med Commun 2016;37(6):593–601.
8. Du Y, Cullum I, Illidge TM, Ell PJ. Fusion of metabolic function and morphology: sequential [18F]fluorodeoxyglucose positron-emission tomography/computed tomography studies yield new insights into the natural history of bone metastases in breast cancer. J Clin Oncol 2007;25(23):3440–3447.
9. Padhani AR, Makris A, Gall P, Collins DJ, Tunariu N, de Bono JS. Therapy monitoring of skeletal metastases with whole-body diffusion MRI. J Magn Reson Imaging 2014;39(5):1049–1078.
10. Walker R, Barlogie B, Haessler J, et al. Magnetic resonance imaging in multiple myeloma: diagnostic and clinical implications. J Clin Oncol 2007;25(9):1121–1128.
11. NICE. Myeloma: diagnosis and management. https://www.nice.org.uk/guidance/ng35/evidence/full-guideline-pdf-2306487277. Published 2016. Accessed October 17, 2019.
12. Dimopoulos MA, Hillengass J, Usmani S, et al. Role of magnetic resonance imaging in the management of patients with multiple myeloma: a consensus statement. J Clin Oncol 2015;33(6):657–664.
13. Padhani AR, Lecouvet FE, Tunariu N, et al. METastasis Reporting and Data System for Prostate Cancer: Practical Guidelines for Acquisition, Interpretation, and Reporting of Whole-body Magnetic Resonance Imaging-based Evaluations of Multiorgan Involvement in Advanced Prostate Cancer. Eur Urol 2017;71(1):81–92.
14. Messiou C, Hillengass J, Delorme S, et al. Guidelines for Acquisition, Interpretation, and Reporting of Whole-Body MRI in Myeloma: Myeloma Response Assessment and Diagnosis System (MY-RADS). Radiology 2019;291(1):5–13.
15. Kosmin M, Makris A, Joshi PV, Ah-See ML, Woolf D, Padhani AR. The addition of whole-body magnetic resonance imaging to body computerised tomography alters treatment decisions in patients with metastatic breast cancer. Eur J Cancer 2017;77:109–116.
16. Zugni F, Ruju F, Pricolo P, et al. The added value of whole-body magnetic resonance imaging in the management of patients with advanced breast cancer. PLoS One 2018;13(10):e0205251.
17. Nakata E, Sugihara S, Osumi S, Yamashita N. Risk stratification for predicting symptomatic skeletal events (SSEs) in breast cancer patients with bone metastases. J Orthop Sci 2017;22(4):743–748.
18. Larbi A, Omoumi P, Pasoglou V, et al. Whole-body MRI to assess bone involvement in prostate cancer and multiple myeloma: comparison of the diagnostic accuracies of the T1, short tau inversion recovery (STIR), and high b-values diffusion-weighted imaging (DWI) sequences. Eur Radiol 2019;29(8):4503–4513.